HYDRAULIC PERFORMANCE OF DOUBLE SLOTTED BARRIERS UNDER REGULAR WAVE ATTACK

E. V. KOUTANDOS
Civil Engineering Department
Technological Educational Institute of Crete
P.O. Box 1939, 71004, Heraklion, Crete
GREECE
ekoutant@gmail.com

Abstract: In the present study, wave interaction with double, fixed, vertical, semi-immersed, slotted barriers is investigated numerically. Numerical results concerning obtained with the use of the COBRAS (Cornell breaking Wave and Structures) wave model for regular waves reveal the effects of barriers porosity, relative depth d/L (d: water depth, L: wave length) and relative distance between the two barriers S/L (S: the distance between the two barriers, L: wave length) on the hydrodynamic characteristics (wave transmission, reflection, dissipation, velocity field, turbulence kinetic energy field). Numerical results concerning wave transmission, reflection, dissipation against the porosity of the barriers, d/L and S/L are well compared with experimental results by Isaacson et al. [14], revealing the credibility of the wave model. Detailed computed velocities and turbulence kinetic energy in the vicinity of the structure indicate the effects of the special breakwater on the flow pattern and the turbulence structure.

Key-Words: - Double Slotted Barriers, Permeable Barriers, Special Breakwater

1 Introduction

Partially immersed breakwaters are among the environmentally friendly coastal structures which may be used for wave protection and restoration of semi-protected coastal regions. They have the advantages of allowing water circulation, fish passage and sediment transport beneath the breakwater. They also may be relatively economical by providing protection closer to the water surface where wave action is more pronounced. In certain situations, breakwaters in the form of thin, rigid, pile supported vertical barriers that extend some distance down from the water surface have been used or considered. Their performance is measured with the wave transmission coefficient C_t ($=H_t/H_i$, H_t=transmitted wave height, H_i= incident wave height) which depends on the ratio B/L (B=structure length, L=wave length) if the structures length B is considerable over the wave length L, the ratio d/L (d=water depth, L=wave length) when the structures length B is not considerable over the wave length L, the structure draught d_r to water depth d ratio (d_r/d, relative draught) and the wave steepness parameter (H_i/gT^2, T=wave period).

In some instances, a permeable barrier, such as a slotted vertical barrier made from timber planks, may be preferred. For example, this may be selected in an effort to reduce unwanted wave reflection on the upwave side of the barrier. A primary feature of such interactions is that wave energy is absorbed within the structure. Permeable barriers have the advantage of reducing wave reflection on the upwave side of the barrier but in order to also reduce wave transmission to an acceptable level it is often necessary to use two vertical barriers in many practical applications.

The study of partially immersed breakwaters has been the focus of many coastal and ocean engineers over some decades. Various analytical, numerical and experimental studies on the wave-structure interaction have been presented in the past.

The hydrodynamic characteristics of partially immersed breakwaters are similar to skirt breakwaters, fixed part-depth screens mounted on piles, Koutandos et al. [6], Koutandos [8]. Under the action of short-period wave trains the structure's draught is the main governing design parameter, leading to increased local turbulence and energy dissipation, Koutandos et al. [7]. Under the action of long period waves where the structure's width tends to be the most important parameter, Koutandos et al. [7], the hydrodynamic response of the two categories of surface piercing structures (fixed or floating) is different.

Analytical studies have been presented for a single thin barrier by Wiegel [23] and for twin thin barriers Wiegel [24]. Wave transmission was underestimated because the effects of wave reflection were neglected, Kriebel [15]. Liu and

Abbaspour [16] used the boundary element method and Reddy and Neelamani [22] a physical model to study wave reflection and transmission characteristics in the vicinity of a rigid thin barrier.

Losada et al. [17] applied linear wave theory in order to examine linear waves impinging obliquely on fixed vertical thin barriers. Theoretical solutions are obtained by an eigenfunction expansion method for the transmission and reflection coefficients. Losada et al. [18] examined modulated waves impinging obliquely on fixed vertical thin barriers. Theoretical solutions are obtained by an eigenfunction expansion method for the transmission and reflection coefficients. Losada et al. [19] applied linear wave theory in order to evaluate the scattering of irregular waves, described by a TMA directional wave spectrum, impinging on fixed vertical thin barriers. The dependence of the transmission and reflection coefficients on the directional spreading function and on the angle of wave incidence was analyzed.

Hagiwara [4] and Bennet et al. [1] presented mathematical models to study the interaction of water waves with a slotted wavescreen breakwater, extending from the free surface to the sea bed. Comparisons with experimental results for transmission and reflection coefficients have been presented in both works.

Isaacson et al. [13] used the eigenfunction expansion method to study the hydrodynamics of a vertical slotted barrier and extended the method to study double slotted barriers, Isaacson et al. [14].

Neelamani & Vedagiri [21] examined experimentally wave interaction with rigid partially immersed twin vertical barriers. Regular and random waves of wide ranges of wave heights, periods and immersions of the structure were examined. Increased energy dissipation was observed in the random waves case.

Koutandos et al. [7] presented an experimental study of waves acting on partially immersed breakwater with four different configurations (single fixed-regular & irregular waves, heave motion free-regular & irregular waves, single fixed with attached front plate-regular waves and double fixed-regular waves) in shallow and intermediate waters. The results showed the effect of the various configurations on the transmission, reflection and energy dissipation coefficients.

Koutandos [9] presented a detailed numerical study on wave interaction with rigid partially immersed slotted vertical barrier. The effects of the relative depth d/L and the porosity of the structure were examined for a wide range of hydrodynamic conditions.

The purpose of this study is to investigate numerically in a 2-dimensional vertical plane (2DV) the hydrodynamic characteristics of double, fixed, vertical, semi-immersed, slotted barriers and the performance of the special breakwater.

2 The numerical model

A brief summary of the governing equations, boundary conditions and solution procedure used in the COBRAS model are presented here, but more details can be found in Liu & Lin (1997).

The unsteady, incompressible RANS (Reynolds Averaged Navier Stokes) equations in a two dimensional vertical plane (2D-V) are solved in conjunction with transport equations for k and ε (Rodi [25]) for the calculation of the Reynolds stresses. The VOF (Volume of Fluid) method (Hirt and Nichols [5]) is used for "tracking" the free surface variation. For each computational cell, a fluid fraction function F is applied, representing the volume fraction of a cell occupied by a fluid. The values of F are in the range of [0,1], with F=1 representing a cell full of fluid, and F=0 a void cell. An unsteady, advection-diffusion equation for a function F, representing the volume fraction of a cell occupied by the fluid, is solved together with the RANS and the k (turbulent kinetic energy) and ε (turbulent dissipation) equations. The donor-acceptor method is used for the free surface reconstruction. The partial cell treatment is used for representing solid objects of arbitrary shape. Similar to the F function, an openness function θ is applied representing the ratio of space not occupied by the solid object to the whole cell area. The values of θ are in the range of [0, 1], with θ=0 representing a solid object and θ=1 an open to the fluid cell, and modified RANS equations are used by including θ in all of the terms.

The solution of the RANS equations is based on the two-step projection method (Chorin [2], [3]) with the use of the finite difference method. The convection terms in the momentum equations are discretized by a combination of the upwind and central difference scheme in order to produce stable and accurate results. The central difference method is used to express the stress gradient and the pressure gradient and the forward time-differencing method for the time derivatives. Similar expressions are used for the k-ε transport equations.

The incident regular wave was generated by the "source function" approach (Lin & Liu [12]) at a distance of 1.5 L from the left side of the domain. The mass source function is applied in a rectangular

source region Ω in the continuity equation, as follows:

$$\frac{\partial U_i}{\partial x_i} = s(i,j,t) \text{ in } \Omega \quad (1)$$

For regular waves the source function is $s(t) = \frac{CH}{A}\sin(\sigma t)$, where C= phase velocity, H=wave height, A= area of the rectangular source region Ω, σ= the wave frequency and t = time. Also a low level of turbulent kinetic energy k is assumed as initial condition in order to maintain stability (Lin & Liu [11]).

The dynamic free surface boundary condition is applied for the mean flow velocities, which is equivalent to the zero stress free surface condition if no stresses are applied on the free surface. For the k and ε the zero normal gradient boundary condition is applied at the free surface, indicating that turbulence does not diffuse across the free surface. At the rigid boundaries (bed and breakwater walls) the no-slip condition is applied and the "wall function" approach is implemented at the first near-wall grid point. This avoids a refined modeling of the viscous sub-layer which would be computationally expensive. Radiation boundary conditions are set at both sides of the computational domain to allow outgoing waves, such as:

$$\frac{\partial R}{\partial t} + C\frac{\partial R}{\partial x} = 0 \quad (2)$$

where R is a wave variable, and C is the phase velocity of the incident regular wave. Additionally a sponge layer is imposed at the left boundary, next to the source function, in order to fully absorb the outgoing waves of different frequencies due to reflection. A sponge layer is an area where an additional friction term of the form $-f(x)\cdot U_i$ is added to the original momentum equation where *f(x)* is a function of distance from the source function (figure 1).

3 Validation of the numerical model Effect of barrier porosity, d/L and S/L

Numerical results concerning reflection and transmission characteristics obtained with the use of the COBRAS wave model for regular waves, are compared with experimental results for double fixed, vertical, semi-immersed, slotted barriers, Isaacson et al. [14]. The effects of the barriers porosity, d/L and S/L on the hydrodynamic characteristics (wave transmission, reflection, dissipation) are investigated.

The physical experiments that are used for comparison purposes were conducted in the wave flume of the Hydraulics Laboratory of the Department of Civil Engineering at the University of British Columbia. The flume was 20 m long and 0.62 m wide. An artificial beach covered by a mat of synthetic hair was located at the downstream end of the flume in order to minimize wave reflection. The permeable wave barrier was constructed of panels such that the porosity of the barrier could vary by changing the dimensions of the slots between the panel members. The barriers were placed in equal distance upwave and downwave from the middle of the flume, 10 m from the wave generator. Three spacings were tested S/L=0.13, 0.33 and 0.66. Half immersed barriers were tested with porosities 0, 0.05 and 0.10. Five different wave periods were tested T=0.6, 0.8, 1.0, 1.2 and 1.4 sec, corresponding to a constant wave steepness, H_i/L=0.07. The water depth was constant in all experiments equal to 0.45 m. Detailed description of the experiments can be found in Isaacson et al. [14].

The set of the experimental results used for validation and in order to examine the effect of the porosity in the performance of the structure includes 3 tests with structure porosity 0, 0.05 and 0.10 under the hydrodynamic conditions described by Isaacson et al. [14], that is d_r/d=0.50 (half immersed barrier), d/L=0.30, S/L=0.33 and H_i/L=0.07. All three physical experiments and two more with porosities 0.15 and 0.20, are reproduced numerically with the use of the COBRAS wave model. A numerical wave tank, with dimensions 20 m x 0.625 m was used. A grid with Δx=0.01 m and Δy=0.005 m is employed resulting in a mesh of 2000x125 grid points. The total computational time for these tests was taken 40T (T: wave period), and the results presented are from 30 T for which numerical stability is achieved, indicated by the total mass and energy in the domain. Each permeable wave barrier was constructed of five solid members of certain height such that the porosity of the barrier could vary by changing the dimensions of the slots between the members.

The numerical wave reflection analysis is based on the method proposed by Mansard and Funke [20]. Energy dissipation in the region of the breakwater is also studied using the following equation proposed by Isaacson et al. [14]:

$C_t^2+C_r^2+C_d=1$ (3)

where C_t is the transmission coefficient (H_t/H_i), C_r is the reflection coefficient (H_r/H_i) and C_d is the energy dissipation coefficient (H_t the height of the transmitted wave, H_r the height of the reflected wave and H_i the height of the incident wave).

Results for C_t (A), C_r (B) and C_d (C) against the porosity are presented in figure 1. The agreement between experimental and numerical results is satisfactory. In figure 1 (A) where C_t is presented it is revealed that wave transmission is proportional to the structure porosity starting from 10% transmission for an impermeable structure (porosity=0) and reaching 70% for porosity=0.2. Therefore it is deduced that the barriers porosity is a very important factor in design, influencing dramatically the efficiency of the structure. On the contrary in figure 1(B) where C_r is presented reflection decreases with the increase of porosity, a fact that contributes to reduce unwanted wave reflection on the upwave side of the barrier. For an impermeable structure (porosity=0) 70% reflection is observed and for porosity=0.2, 20%. In figure 1(C) the variation of C_d is presented. Higher values are observed for the 0.05 porosity barriers case, due to the stronger wave-structure interaction in the specific case. Dissipation is minimum for the highest porosity examined 0.2 since wave energy is easily allowed to be transmitted downwave the barrier.

The set of the experimental results used for validation and in order to examine the effect of d/L in the performance of the structure includes 5 tests (T=0.6, 0.8, 1.0, 1.2 and 1.4 sec) with structure porosity 0.05, d_r/d=0.50 (half immersed barrier), d/L=0.30, S/L=0.33 and H_i/L=0.07. In figure 2 numerical results for C_t (A), C_r (B) and C_d (C) are presented against d/L. The influence of d/L (d=the water depth) on the performance of the structure is shown. Transmission decreases with increase of d/L revealing the fact that the structure is more efficient in deeper waters. Substantial protection is offered by the structure for all cases examined since C_t<0.50 for all cases examined, d/L>0.15. It is also expected that the efficiency of the structure will be greater in deeper waters. The inverse variation is observed in reflection coefficient C_r case, in figure 2 (B). The reflection coefficient C_r increases with increase of d/L starting from 15% for d/L=0.15 and reaching 65% for d/L=0.80. The energy dissipation coefficient C_d which is presented in figure 2 (C), follows the trend of the other two energy coefficients since it is provided using equation (3). Higher values are observed for d/L<0.30, where wave reflection is lower.

The set of the experimental results used for validation and in order to examine the effect of S/L in the performance of the structure includes 3 tests (S/L=0.13, 0.33 and 0.66) with structure porosity 0.05, d_r/d=0.50 (half immersed barrier), d/L=0.30, S/L=0.33 and H_i/L=0.07. In figure 3 numerical results for C_t (A), C_r (B) and C_d (C) are presented against S/L. Measured and predicted hydrodynamic coefficients compare reasonably well for all three barrier spacings. The influence of S/L on the performance of the structure is shown. Transmission decreases slightly with increase of S/L from 28% for S/L=0.13 to 23% for S/L=0.66 corresponding to resonant excitation of partial standing waves between the barriers that lead to a reduction in the energy dissipation coefficient as noted by Isaacson et al. [14] and Koutandos et al. [7]. The inverse variation is observed in reflection coefficient C_r case, in figure 3 (B). The reflection coefficient C_r increases slightly with increase of d/L starting from 44% for S/L=0.13 and reaching 47% for S/L=0.66. The energy dissipation coefficient C_d which is presented in figure 3 (C), follows the trend of the other two energy coefficients since it is provided using equation (3). Slightly higher values are observed for the two lower S/L values, where wave reflection is lower.

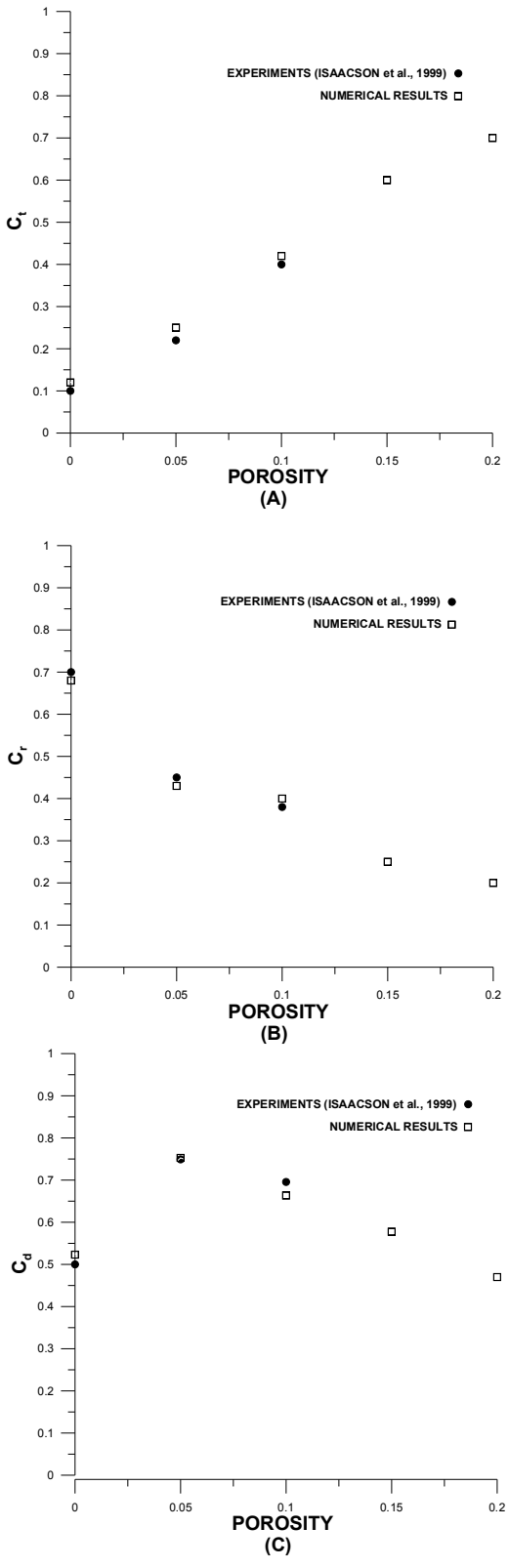

Figure 1. Comparison between experimental Isaacson et al. (1999), and numerical results for C_t, C_r and C_d against porosity of the slotted barrier.

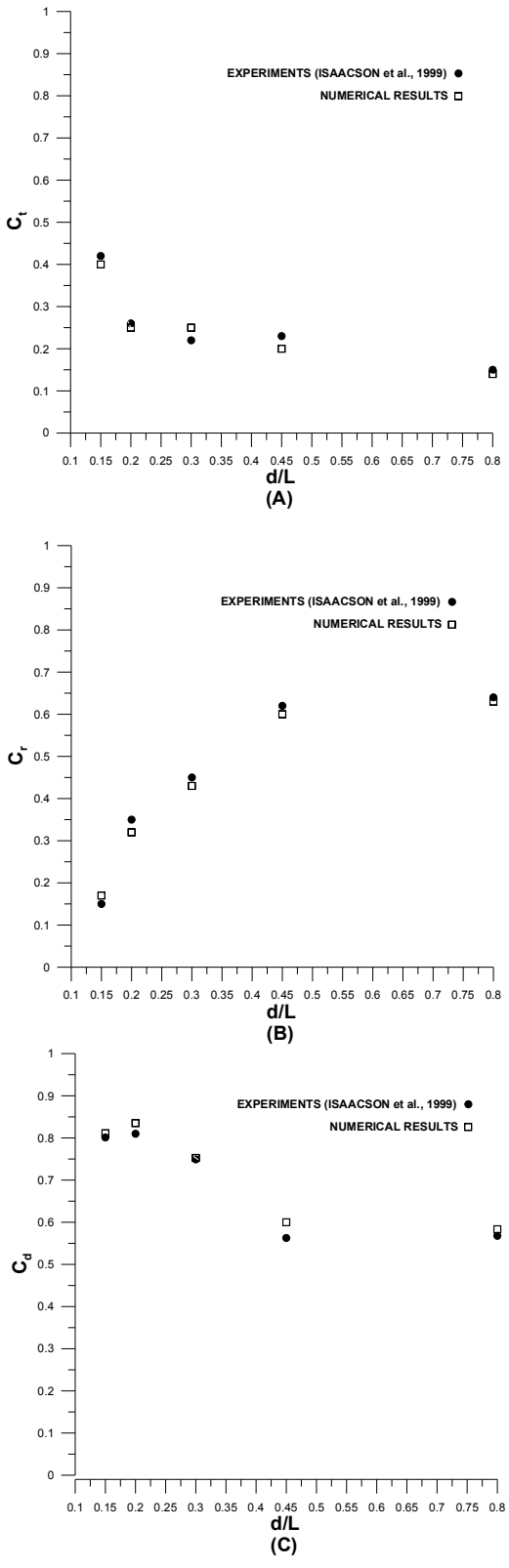

Figure 2. Comparison between experimental Isaacson et al. (1999), and numerical results for C_t, C_r and C_d against d/L.

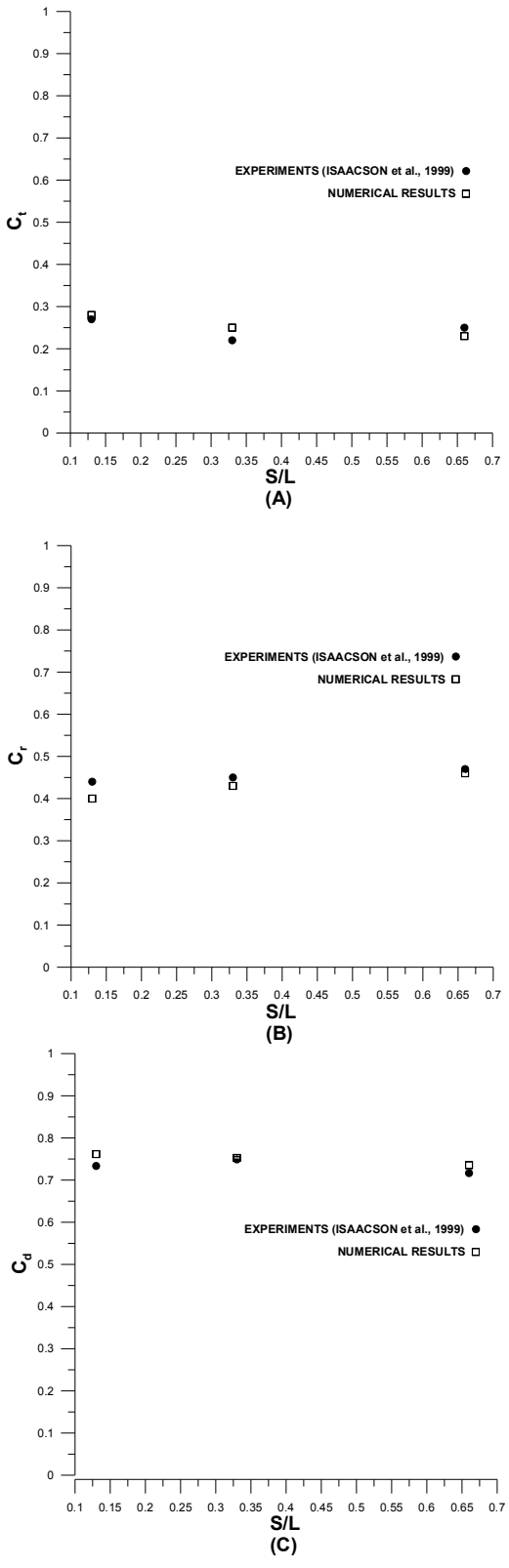

Figure 3. Comparison between experimental Isaacson et al. (1999), and numerical results for C_t, C_r and C_d against S/L.

4 Mean velocity and turbulence kinetic energy fields

The set of the experimental results used in order to examine the effect of the porosity in mean velocity and turbulence kinetic energy fields includes 3 tests with structure porosity 0, 0.10 and 0.20 for d_r/d=0.50 (half immersed barrier), d/L=0.30, S/L=0.66 and H_i/L=0.07. The highest value of the S/L ratio is used in order to examine in detail the dynamic behavior of the water mass included between the two barriers.

The mean velocity field in the breakwater area is presented in figure 4 (A)-t=30.25T, (B)-t=30.50T and (C)-t=30.75T over the 30th wave cycle for porosity=0.0, in figure 5 (A)-t=30.25T, (B)-t=30.50T and (C)-t=30.75T for porosity=0.1 and figure 6 (A)-t=30.25T, (B)-t=30.50T and (C)-t=30.75T for porosity=0.2. Maximum velocities 1.00 m/s are observed in the region of the impermeable barriers (figure 4) and mainly in the seaward side of the structures where the main structure-interaction takes place and intense vortices are observed. A recirculating region is observed in the region beneath the body of each barrier with the first one being stronger and wider. In figure 5 the mean velocity field for permeable barrier with porosity 0.10 is presented. Maximum velocities appear also in the region of the barriers but reach the value of 0.60 m/s lower than the maximum velocity observed in the impermeable barriers case under the same hydrodynamic conditions. The recirculating region this time is obvious only beneath the first barrier while the interaction of the water mass with the gaps on the body of the barriers is presented. The highest maximum velocities observed are presented in the maximum porosity case examined 0.20 where they reach the value of 1.20 m/s. The recirculating region this time is slightly obvious only beneath the first barrier while the interaction of the water mass with the gaps on the body of the barriers is much more intense than the previous case.

In all three cases examined the existence of partially standing waves in the region between the two barriers is revealed.

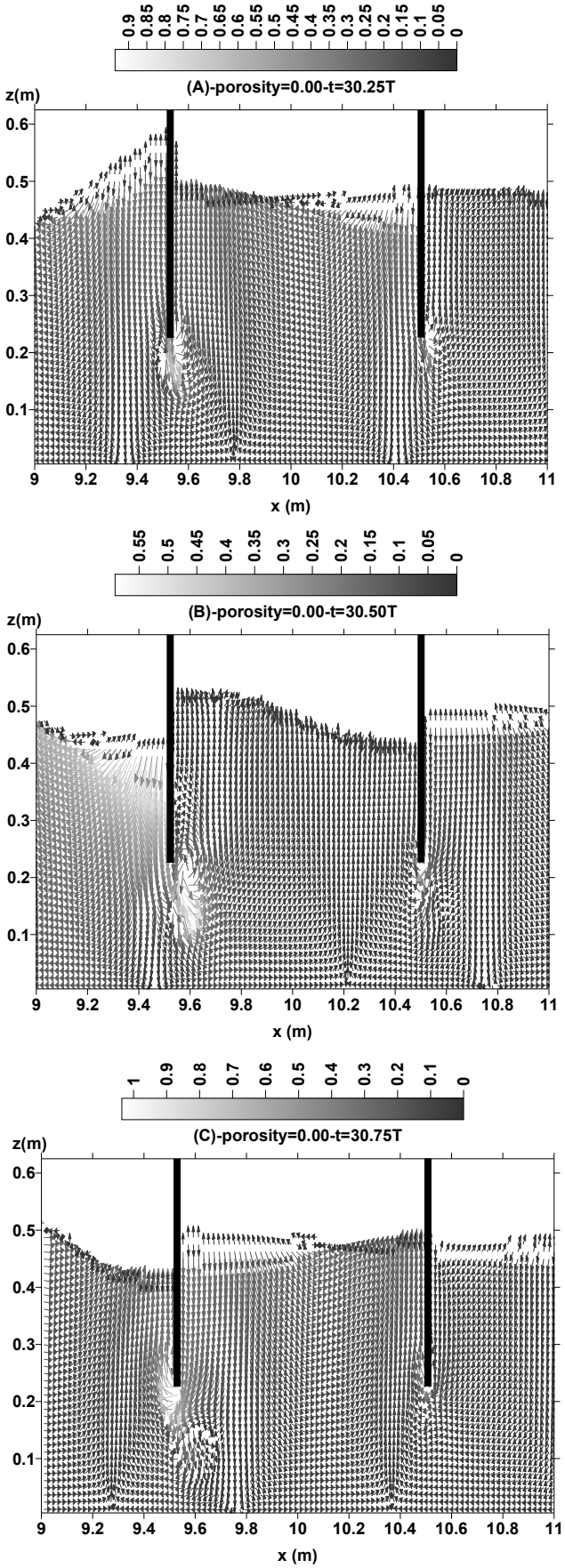

Figure 4. Detailed velocity field in the region of the barriers (Porosity=0.00, H_i=0.1 m-T=1.00 sec).

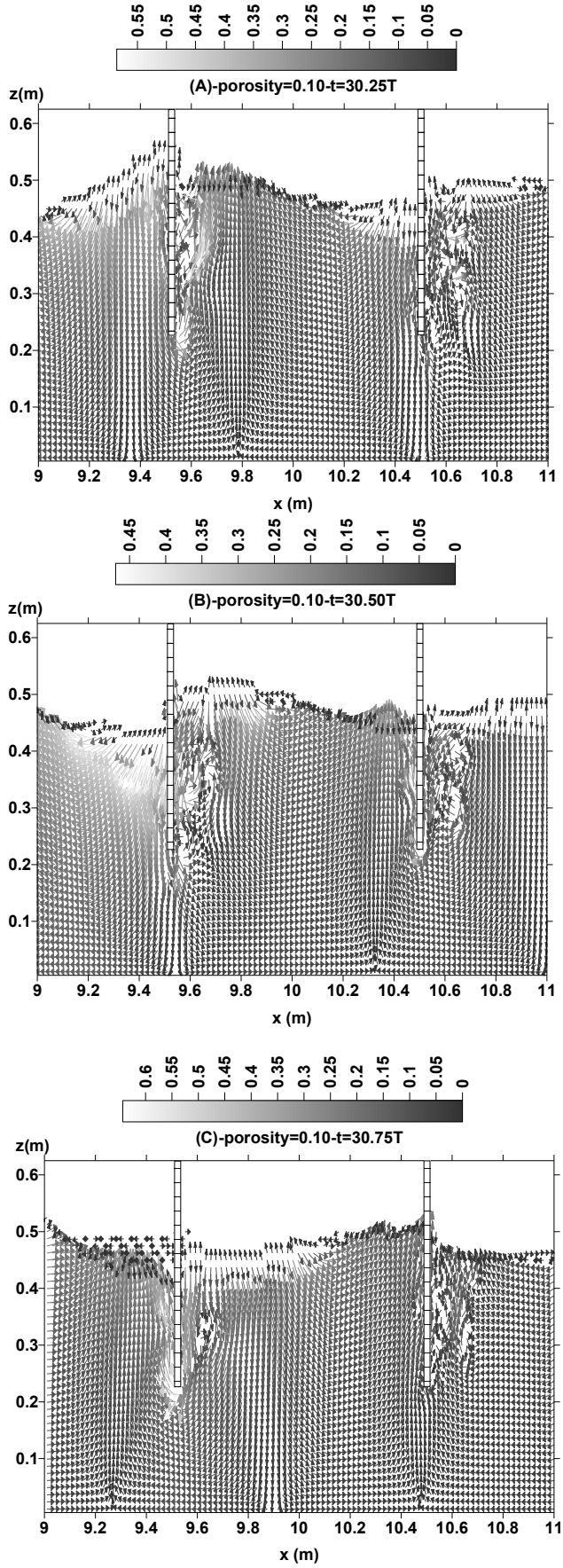

Figure 5. Detailed velocity field in the region of the barriers (Porosity=0.10, H_i=0.1 m-T=1.00 sec).

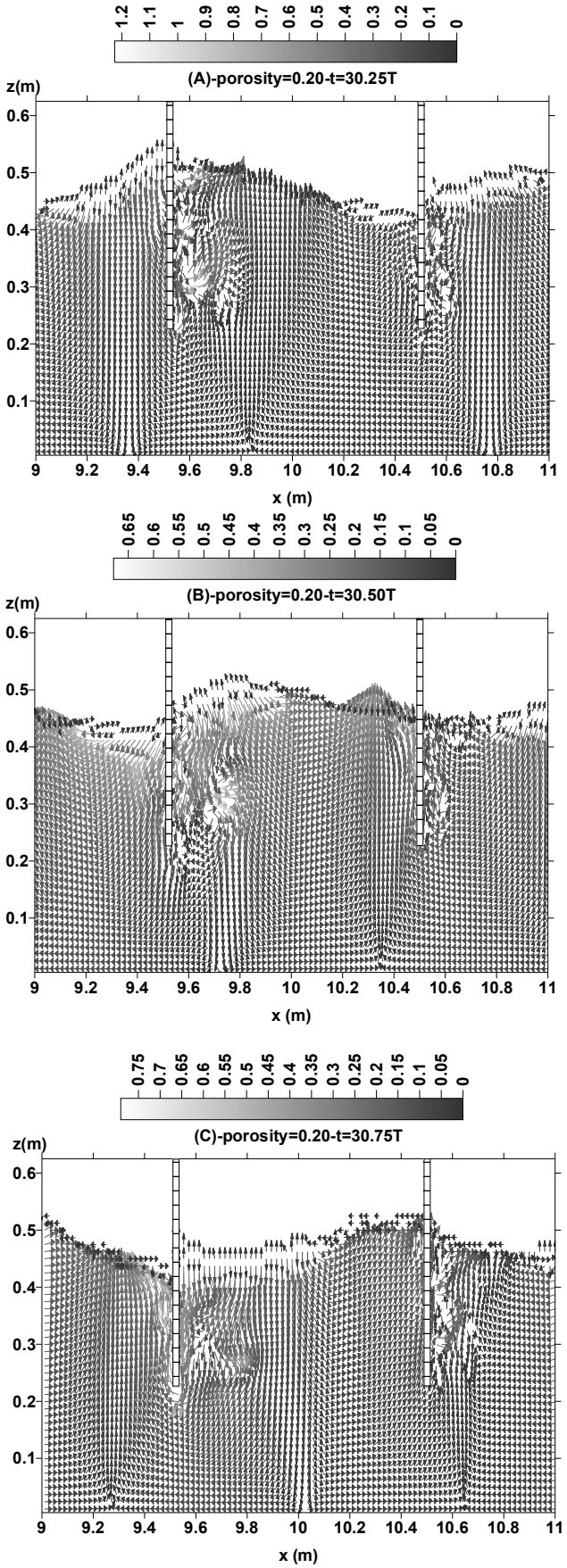

Figure 6. Detailed velocity field in the region of the barriers (Porosity=0.20, H_i=0.1 m-T=1.00 sec).

The turbulence kinetic energy ($\sqrt{2k}$) in the breakwater area is presented in figure 7 (A)-t=30.25T, (B)-t=30.50T and (C)-t=30.75T over the 30th wave cycle for porosity=0.0, in figure 8 (A)-t=30.25T, (B)-t=30.50T and (C)-t=30.75T over the 30th wave cycle for porosity=0.1 and in figure 9 (A)-t=30.25T, (B)-t=30.50T and (C)-t=30.75T over the 30th wave cycle for porosity=0.2.

In figure 7 the turbulence kinetic energy ($\sqrt{2k}$) field in the region of the impermeable barriers area is presented. Maximum values of turbulence kinetic energy ($\sqrt{2k}$) (0.15 m/s) are observed in the region of the first and second barrier and mainly in the submerged edges of the barriers where the main wave-structure interaction takes place and intense oscillating vortices around the submerged edges of the barrier are observed. The form and the area of these vortices are not constant in time but variable presenting nevertheless almost constant average maximum values of turbulence kinetic energy. Highest values are observed right beneath the submerged edges of the barriers extending to a certain distance, forming cycles of lowering intensity as we move away from the barriers. It is obvious due to the intensity and the form of these vortices that the main interaction takes place with the first barrier.

In figure 8 the turbulence kinetic energy ($\sqrt{2k}$) field in the region of the permeable barriers (porosity 0.10) area is presented. Maximum values of turbulence kinetic energy ($\sqrt{2k}$) reach the value of 0.47 m/s and are greater than the impermeable barrier case. This time maximum values are observed in the region of the main body of the barriers, especially the first one, and mainly in the upper part near the free surface. Highest values are observed in the slots of the body of the barriers and mainly in the upper part near the free surface where wave action is more pronounced.

In figure 9 the turbulence kinetic energy ($\sqrt{2k}$) field in the region of the permeable barrier (porosity 0.20) area is presented. Maximum values of turbulence kinetic energy ($\sqrt{2k}$) reach the value of 0.63 m/s and are much higher than all the other cases examined. Maximum values are observed in the region of the lower part of the main body of the first barrier and more specifically in the slots of the body of the barrier and right behind them.

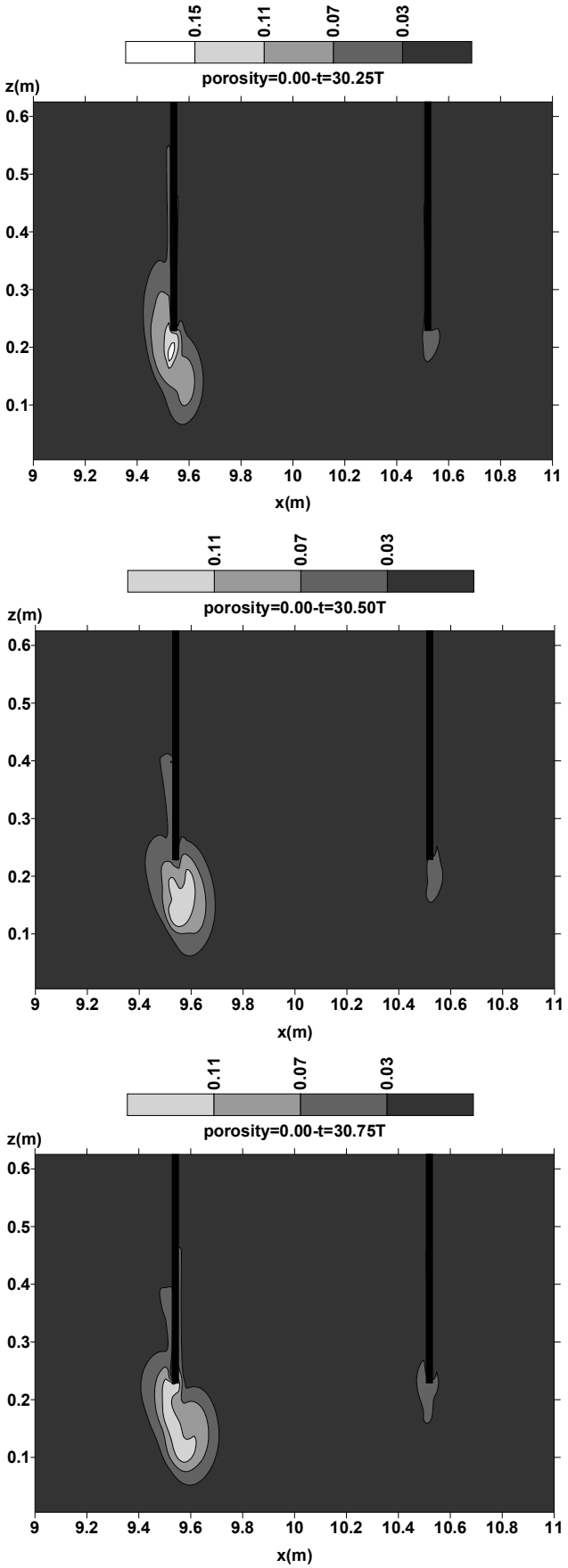

Figure 7. $\sqrt{2k}$ field in the region of the barriers (Porosity=0.00, H_i=0.1 m-T=1.00 sec).

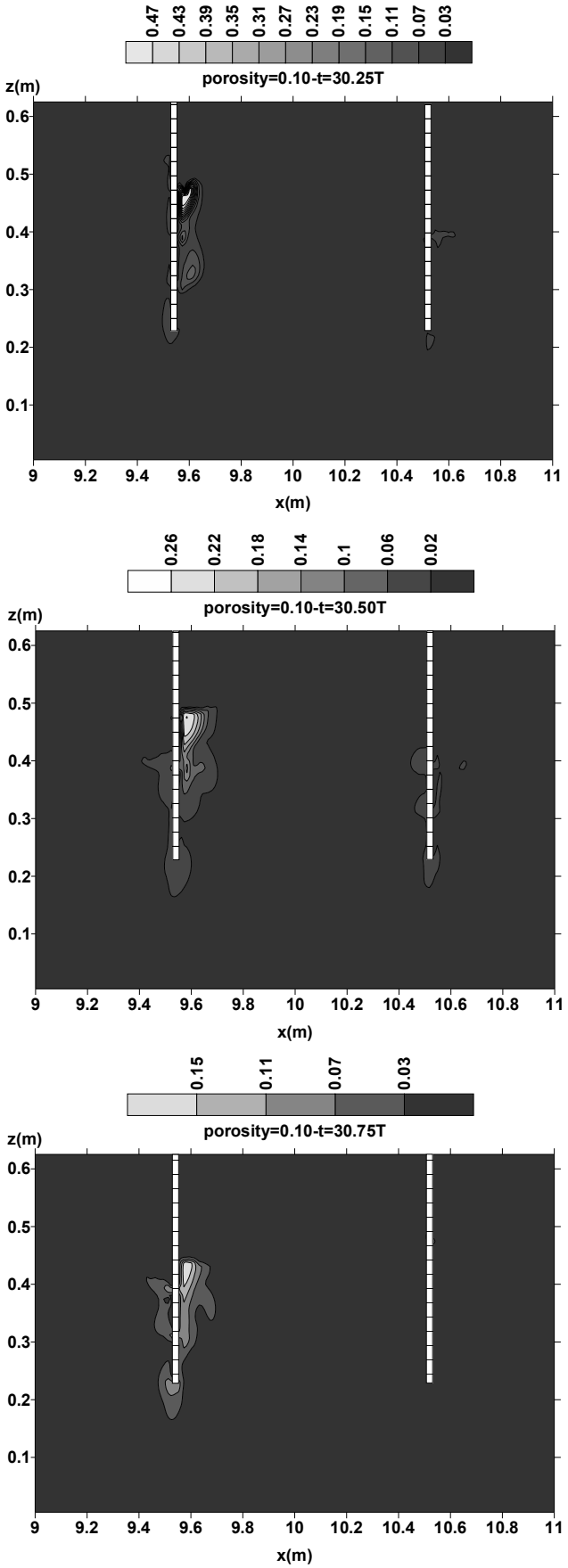

Figure 8. $\sqrt{2k}$ field in the region of the barriers (Porosity=0.10, H_i=0.1 m-T=1.00 sec).

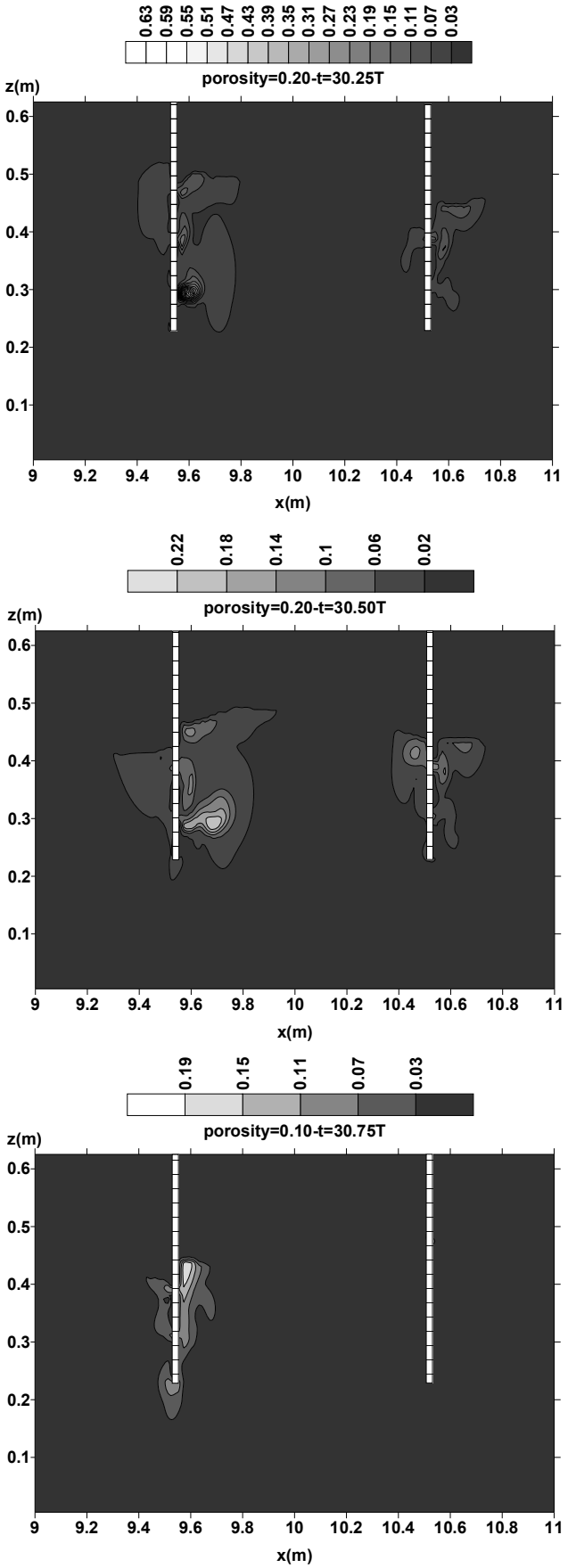

Figure 9. $\sqrt{2k}$ field in the region of the barriers (Porosity=0.20, H_i=0.1 m-T=1.00 sec).

5 Conclusions

In the present study, wave interaction with double, fixed, vertical, semi-immersed, slotted barriers is investigated numerically. Numerical results concerning obtained with the use of the COBRAS (Cornell breaking Wave and Structures) wave model for regular waves reveal the effects of barriers porosity, relative depth d/L (d: water depth, L: wave length) and relative distance between the two barriers S/L (S: the distance between the two barriers, L: wave length) on the hydrodynamic characteristics (wave transmission, reflection, dissipation, velocity field, turbulence kinetic energy field). Numerical results concerning wave transmission, reflection, dissipation against the porosity of the barriers, d/L and S/L are well compared with experimental results (Isaacson et al., 1999) revealing the credibility of the wave model. Detailed computed velocities and turbulence kinetic energy in the vicinity of the structure indicate the effects of the special breakwater on the flow pattern and the turbulence structure.

The following conclusions can be derived:

- Wave transmission is proportional to the structure porosity starting from 10% transmission for an impermeable structure (porosity=0) and reaching 70% for porosity=0.2 under certain hydrodynamic conditions. Therefore it is deduced that the barrier porosity is a very important factor in design influencing dramatically the efficiency of the structure.
- Wave reflection decreases with the increase of porosity, a fact that contributes to reduce unwanted wave reflection on the upwave side of the barrier. For an impermeable structure (porosity=0) 70% reflection is observed and for porosity=0.2, 20% under certain hydrodynamic conditions.
- The highest values for energy dissipation are observed for the 0.05 porosity barriers case, due to the stronger wave-structure interaction in the specific case. Dissipation is minimum for the highest porosity examined 0.2 since wave energy is easily allowed to be transmitted downwave the barriers.
- Transmission decreases with increase of d/L for all porosities examined revealing the fact that the structure is more efficient in deeper waters. Substantial protection is offered by the structure for all cases examined for porosity=0.05 since C_t<0.50

for all cases examined, d/L>0.15. It is also expected that the efficiency of the structure will be greater in deeper waters. Reflection increases with increase of d/L starting from 15% for d/L=0.15 and reaching 65% for d/L=0.80..

- For energy dissipation, higher values are observed for d/L<0.30, where wave reflection is lower.
- Transmission decreases slightly with increase of S/L from 28% for S/L=0.13 to 23% for S/L=0.66 corresponding to resonant excitation of partial standing waves between the barriers that lead to a reduction in the energy dissipation coefficient.
- The inverse variation is observed in reflection coefficient C_r case. The reflection coefficient C_r increases slightly with increase of d/L starting from 44% for S/L=0.13 and reaching 47% for S/L=0.66.
- Slightly higher values for the energy dissipation coefficient are observed for the two lower S/L values, where wave reflection is lower.
- Maximum velocities 1.00 m/s are observed in the region of the impermeable barriers and mainly in the seaward side of the structures where the main structure-interaction takes place and intense vortices are observed. A recirculating region is observed in the region beneath the body of each barrier with the first one being stronger and wider. Maximum velocities for permeable barriers with porosity 0.1, appear also in the region of the barriers but reach the value of 0.60 m/s lower than the maximum velocity observed in the impermeable barriers case under the same hydrodynamic conditions. The recirculating region this time is obvious only beneath the first barrier while the interaction of the water mass with the gaps on the body of the barriers is presented. The highest maximum velocities observed are presented in the maximum porosity case examined 0.20 where they reach the value of 1.20 m/s. The recirculating region this time is slightly obvious only beneath the first barrier while the interaction of the water mass with the gaps on the body of the barriers is much more intense than the previous case. In all three cases examined the existence of partially standing waves in the region between the two barriers is revealed.
- For the impermeable barriers case maximum values of turbulence kinetic energy ($\sqrt{2k}$) (0.15 m/s) are observed in the region of the first and second barrier and mainly in the submerged edges of the barriers where the main wave-structure interaction takes place and intense oscillating vortices around the submerged edges of the barrier are observed. The form and the area of these vortices are not constant in time but variable presenting nevertheless almost constant average maximum values of turbulence kinetic energy. Highest values are observed right beneath the submerged edges of the barriers extending to a certain distance, forming cycles of lowering intensity as we move away from the barriers. It is obvious due to the intensity and the form of these vortices that the main interaction takes place with the first barrier. For the permeable barriers (porosity 0.10) maximum values of turbulence kinetic energy ($\sqrt{2k}$) reach the value of 0.47 m/s and are greater than the impermeable barrier case. This time maximum values are observed in the region of the main body of the barriers, especially the first one, and mainly in the upper part near the free surface. Highest values are observed in the slots of the body of the barriers and mainly in the upper part near the free surface where wave action is more pronounced. For the permeable barrier (porosity 0.20) maximum values of turbulence kinetic energy ($\sqrt{2k}$) reach the value of 0.63 m/s and are much higher than all the other cases examined. As in the previous case maximum values are observed in the region of the main body of the barriers. Highest values are observed in the slots of the body of the barriers, mainly in the lower part of the structure body.

LIST OF NOTATION

A: area of the rectangular source region Ω
B : structure length
C: wave phase velocity
C_t : transmission coefficient (H_t/H_i)
C_r : transmission coefficient (H_r/H_i)
C_d : energy dissipation coefficient
d_r: structure draught
d : water depth
dx: horizontal resolution
dy: vertical resolution
F: fluid fraction function (volume fraction of a computational cell occupied by a fluid)
H_t : transmitted wave height
H_r : reflected wave height
H_i : incident wave height
H_s : significant wave height (irregular waves)
k : turbulent kinetic energy
L: wave length
R: wave variable
S: distance between the two barriers
t: time
T: wave period
U_i: velocity
x : horizontal distance
y: vertical distance
ε: turbulent dissipation
θ: openness function (the ratio of space not occupied by the solid object to the whole computational cell area)
σ: wave frequency
Ω: rectangular source region

References:

[1] X1. Bennet, G. S., McIver, P., Smallman, J. V., A mathematical model of a slotted wavescreen breakwater, *Coastal Engineering*, Vol. 18, 1993, pp. 231-249.

[2] X2. Chorin, A.J., Numerical solution of the Navier-Stokes equations, *Math. Comp.*, Vol. 22, 1968, pp.745-762.

[3] X3. Chorin, A.J., On the convergence of discrete approximations of the Navier-Stokes equations, *Math. Comp.*, Vol. 23, 1969, pp. 341-353.

[4] X4. Hagiwara, K., Analysis of upright structure for wave dissipation using integral equation, *Proceedings of the 19th Coastal Engineering Conference*, ASCE, Vol. 3,1984, pp. 2810-2826.

[5] X5. Hirt, C.W. and Nichols, B.D., Volume of Fluid (VOF) Method for the Dynamics of Free Boundaries, *Journal of Computational Physics*, Vol. 39, 1981, pp. 201-225.

[6] X6. Koutandos E.V., Karambas Th.V., Koutitas C.G., Floating breakwater response to waves action using a Boussinesq model coupled with a 2dv elliptic solver, *Journal of Waterway, Port, Coastal and Ocean Engineering*, ASCE, Vol. 130, 2004, pp.243-255.

[7] X7. Koutandos, E., Prinos, P. and Gironella, X., Floating breakwaters under regular and irregular wave forcing-Reflection and transmission characteristics, *Journal of Hydraulic Research*, IAHR, Vol. 43, 2005, pp.174-188.

[8] X8. Koutandos E.V., Hydrodynamic analysis of a skirt breakwater, *Journal of Maritime Engineering*, ICE, Vol. 160, Issue MA3, 2007, pp. 121-133.

[9] X9. Koutandos E.V., Hydrodynamics of vertical semi-immersed slotted barrier, *WSEAS Transactions on Fluid Mechanics*, Volume 4, Issue 3, 2009, pp. 85-96.

[10] X10. Liu, L.-F. P. and Lin, P., A numerical model for breaking waves: The Volume of Fluid Method, *Research Report. No. CACR-97-02*, Center for Applied Coastal Research, Ocean Engineering Laboratory, University of Delaware, 1997.

[11] X11. Lin, P. and Liu, L.-F. P., A numerical study of breaking waves in the surf zone, *Journal of Fluid Mechanics*, Vol. 359, 1998, pp. 239-264.

[12] X12. Lin, P. and Liu, L.-F. P., Internal wave-maker for Navier-Stokes equation models. *Journal of Waterway, Port, Coastal and Ocean Engineering*, Vol. 125, 1999, pp. 207-215.

[13] X13. Isaacson, M., Premasiri, S., Yang, G., Wave interactions with vertical slotted barriers, *Journal of Waterway, Port, Coastal and Ocean Engineering*, ASCE, Vol.124, 1998, pp. 479-491.

[14] X14. Isaacson, M., Baldwin, J., Premasiri, S., Yang, G., Wave interactions with double slotted barriers, *Applied Ocean Research*, Vol. 21, 1999, pp. 81-91.

[15] X15. Kriebel, D.L., Vertical wave barriers: wave transmission and wave forces, *Proceedings of 23rd Coastal Engineering Conference*, ASCE, Vol. 2, 1992, pp.1313-1326.

[16] X16. Liu P.-L.F., Abbaspour M., Wave scattering by a rigid thin barrier, *Journal of Waterway, Port, Coastal and Ocean Engineering*, ASCE, Vol. 108, 1982, pp. 479-491.

[17] X17. Losada I.J., Losada M.A., Roldan A.J., Propagation of oblique incident waves past rigid vertical thin barriers, *Applied Ocean Research*, Vol. 14, 1992, pp. 191-199.

[18] X18. Losada M.A.., Losada I.J., Roldan A.J., Propagation of oblique incident modulated waves past rigid, vertical, thin barriers, *Applied Ocean Research*, Vol. 15, 1993, pp. 305-310.

[19] X19. Losada M.A., Losada I.A., Losada R., Wave spectrum scattering by vertical thin barriers,

Applied Ocean Research, Vol. 16, 1994, pp.123-128.
[20] X20. Mansard, E.P.D., Funke, E.R., The measurement of incident and reflected spectra using a least squares method, *Proc. 17th Coastal Engineering Conference*, ASCE, Vol. 1, 1980, pp. 154-172.
[21] X21. Neelamani, S. and Vedagiri, M., Wave interaction with partially immersed twin vertical barriers, *Ocean Engineering*, Vol.20, 2002, pp. 215-238.
[22] X22. Reddy M.S., Neelamani S., Wave transmission and reflection characteristics of a partially immersed rigid vertical barrier, *Ocean Engineering*, Vol. 19, 1992, pp.313-325.
[23] X23. Wiegel R.L., Transmission of waves past a rigid vertical thin barrier, *Journal of Waterways and Harbors Division*, ASCE, Vol. 86, 1960, paper 2413.
[24] X24. Wiegel R.L., Closely spaced piles as a breakwater, *Dock and Harbor Authority*, Vol. 42 (491), 1961, 150.
[25] X25. Rodi W., Turbulence models and their application in hydraulics-A State of the art review, *IAHR publication*, Delft, Neteherlands, 1980.